Quantum Electronics **40** (4) 288 – 295 (2010)

INVITED PAPER

PACS numbers: 42.65.Yj; 42.70.Mp; 42.79.Jq; 77.84.Bw
DOI: 10.1070/QE2010v040n04ABEH014237

Investigation into the ways of tuning parametric oscillators of visible and IR ranges*

S.A. Andreev, N.P. Andreeva, M.S. Barashkov, V.V. Badikov, V.K. Demkin, A.K. Don, V.M. Epikhin, M.I. Krymskii, Yu.K. Kalinnikov, K.V. Mitin, A.M. Seregin, V.V. Sinaiskii, M.A. Talalaev, A.A. Chistyakov, N.I. Shchebetova, T.A. Shchetinkina

Abstract. **Different versions of optical parametric oscillator (OPO) schemes were experimentally realised and investigated, which utilise $AgGaS_2$, $LiNbO_3$, and $HgGa_2S_4$ single crystals as well as an $Hg_{1-x}Cd_xGa_2S_4$ solid solution. The OPOs generate radiation in the 1.2 – 5.7-μm range and make use of different ways of output wavelength tuning, including fast wavelength tuning (in a time shorter than 0.1 ms) with the help of an acoustooptical deflector. The output spectral line was narrowed by means of an intracavity acoustooptical filter. An OPO for the visible range with an electrodynamic tuning to an arbitrary wavelength in this range in a time of 5 ms was implemented employing a BBO single crystal.**

Keywords: *optical parametric oscillator, wavelength tuning, acoustooptical deflector, acoustooptical filter, electrodynamic driver.*

1. Introduction

At present, nonlinear-optical frequency conversion in optical parametric oscillators (OPOs) is one of the most promising ways of generating high-energy radiation in the visible and IR spectral ranges. Frequency tuneable OPOs show promise for the solution of a variety of problems, including special ones. Examples of the spectroscopic application of wide-band OPOs are provided by the CARS process as well as by coherent intracavity spectroscopy and incoherent femto- and picosecond spectroscopy [1, 2]. Narrow-band probe radiation sources are required in the making of efficient and multi-purpose (intended for a large set of substances under detection) differential absorption (DA) systems [3, 4].

The development of near-IR (0.7 – 2.5 μm), middle-IR (2.5 – 11 μm) and visible-range OPOs, which was pursued in the 'Astrofizika' Research and Production Association for over last ten years, was aimed both at increasing the rate and range of tuning and at extending them to the middle-IR range.

One of essential requirements imposed on OPOs operating in mobile DA lidars is the high rate of tuning. In Ref. [5] we developed the concept of a dual-range OPO-based IR radiator for checking the leak proofness of delivery ducts and gas storages, estimating the loss of hydrocarbon raw stock, and identifying the explosion hazard of a leak cloud. The technical solution implied the operation of an OPO-based gas analyser in two hydrocarbon absorption ranges: in the range of strong (near 3.3 μm) and weak (near 1.66 μm) absorption. Techniques were under development to improve the OPO speed of response by employing electrodynamic drivers (with a switching time of 5 ms), acoustooptical deflectors (AODs) (with a switching time of 0.1 ms), as well as acoustooptical filters (AOFs), which allows tuning within the OPO emission line [6].

The OPO advancement to the middle IR range took place due to the development of chalcogenide single crystal growth technology in the High Technologies Laboratory of Kuban State University. In particular, it has been possible to grow the crystal (solid solution) of cadmium – mercury thiogallate ($Hg_{1-x}Cd_xGa_2S_4$) with a high optical quality and a smoothly varying cadmium density in the plane of phase matching [7 – 9].

2. OPO with a 'fast' frequency tuning

2.1 OPO with a $LiNbO_3$ single crystal and acoustooptical control over the output spectrum

Experimental facility. Figure 1 is a diagrammatic representation of the experiment. Shown is an OPO with an intracavity AOF location, although in several experiments the filter was placed outside of the cavity. To protect the cavity mirrors and the intracavity selective elements, for instance the AOF, against direct exposure to the high-power pump radiation, the OPO cavity with a $LiNbO_3$ single crystal and a feedback for the longest-wavelength radiation employed a noncollinear setup. The pump laser (*1*) possessed the following parameters: $\lambda = 1.064$ μm, a

* Devoted to the 40th anniversary of 'Astrofizika' Research and Production Association.

S.A. Andreev, N.P. Andreeva, M.S. Barashkov, V.K. Demkin, A.K. Don, M.I. Krymskii, K.V. Mitin, A.M. Seregin, V.V. Sinaiskii, M.A. Talalaev, N.I. Shchebetova, T.A. Shchetinkina 'Astrofizika' Research and Production Association, Volokolamskoe sh. 95, 123424 Moscow, Russia; e-mail: np_andreeva@mail.ru, aphysica@aha.ru;
V.V. Badikov High Technologies Laboratory, Kuban State University, ul. Stavropol'skaya 149, 350058 Krasnodar, Russia; e-mail: ntlab@mail.kubsu.ru;
V.M. Epikhin, Yu.K. Kalinnikov All-Russia Research Institute of Physicotechnical and Radio Engineering Measurements, 141570 Mendeleevo, Moscow Region, Russia; e-mail: office@vniiftri.ru;
A.A. Chistyakov National Research Nuclear University 'MEPhI', Kashirskoe sh. 31, 115409 Moscow, Russia; e-mail: chistaa@mail.ru

Received 9 October 2009; revision received 5 March 2010
Kvantovaya Elektronika **40** (4) 288 – 295 (2010)
Translated by E.N. Ragozin

pulse energy of up to 1.4 J, a pulse length of 9 ns, a pulse repetition rate of 10 Hz, a uniform and nearly rectangular intensity distribution profile. The radiation of the pump laser (*1*) transmitted through an AOD (*2*) was directed by deflecting mirrors (*3*) onto a nonlinear crystal (*6*) ($LiNbO_3$) at angles α varied with the help of an AOD (*2*) in the range $3.2^\circ - 6.4^\circ$ in the air. The cavity was tuned to the long-wavelength range of lasing with $R = 99\,\%$ [mirror (*5*)] and $R = 91$ % [mirror (*11*)]. The AOF unit (*10*) was placed either inside the cavity – for generating narrow-band radiation, or outside of it – for the extracavity measurement of the natural OPO lasing width. To this end, the scheme was modified: the AOF (*10*) was placed in front of a spectrometer (*13*). The AOF was controlled by a driver (*15*) and synchronised with the pump generator using a G5-54 oscillator (*14*), which produced pulses of desired duration ($\tau_p = 180$ μs) with a time delay of $\tau_d = 150$ μs. The output radiation power was measured with a PE-25BB energy meter with a NOVA recorder (*12*).

The lasing wavelength was measured with a Digikrom CM 112 spectrometer (*13*) and visualised with a sum frequency generator (SFG), which converted the radiation of the 1.5–1.8 μm wavelength range to 0.61–0.65 μm radiation by focusing, with the help of a lens (*7*), the radiation with ω_{idle} and ω_p onto a 25-mm-long KTA crystal (*8*), whose optical axis made an angle of 53° with the normal to its input face. In the crystal there occurred frequency summation, i.e. the nonlinear IR radiation conversion to the red spectral range. The visible radiation illuminated the slit (*20*) of a spectral analyser (*17*) via an optical fibre bundle (*21*). The visualised radiation was recorded with a WAT-502A video camera, and the video signal from the camera was observed using a picture monitor (*19*) in the form of the image of a vertical slit (*20*). In the upper part of the screen there was the image of 0.6328-μm reference radiation, while in its central part there was the horizontally moving radiation under study. The monitor screen measured 68 mm horizontally; the measured screen scale was 1 cm^{-1} mm^{-1}, which permitted measuring the lasing wavelength to within 1 cm^{-1}.

OPO frequency tuning with the help of an AOD. The main technical characteristics of the TeO_2 crystal based AOD employed in our experiment were as follows: an angular scanning range of $\pm 1^\circ$, an optical transfer coefficient of no less than 90 %, a prescribed wavelength setting time of ~ 0.1 ms, a depolarisation degree below 5 %, an electronic frequency tuning range of 70–90 MHz, the frequency was changed with a discreteness of 80 (roughly) and 1000 (accurately). The AOD was controlled with a personal computer with a built-in LA-2TsAP15 board and the corresponding software.

The AOD-assisted OPO tuning was investigated for an extracavity position of the AOF. The horizontally polarised radiation of the single-mode Nd:YAG pump laser (*1*) ($\lambda_p = 1.064$ μm) was fed to the OPO by mirrors (*3*) via the AOD cell (*2*). The pump pulse duration was equal to 10 ns and the pulse energy was 250 mJ. The scanning was performed in the 1° range, which theoretically corresponded to a spectral tuning range of 2.8–3.4 μm. The OPO unit was assembled according to a noncollinear scheme with a minimal noncollinearity angle $\alpha = 3.2^\circ$ between the cavity axis and the pump radiation direction. Figure 2 shows the tuning curves and experimental points; the AOD acoustic frequency ranged from 73.1 to 83.5 MHz; in this case, the OPO lasing wavelengths were tuned in the ranges 1.56–1.69 μm and 3.36–2.88 μm. The $LiNbO_3$ crystal was stationary, its optical axis made an angle of 48.5° with the cavity axis, and the noncollinearity angle α varied from 4° to 5°.

The further expansion of the angular spectral tuning range was limited by the departure of the pump radiation from the interaction region in the nonlinear crystal.

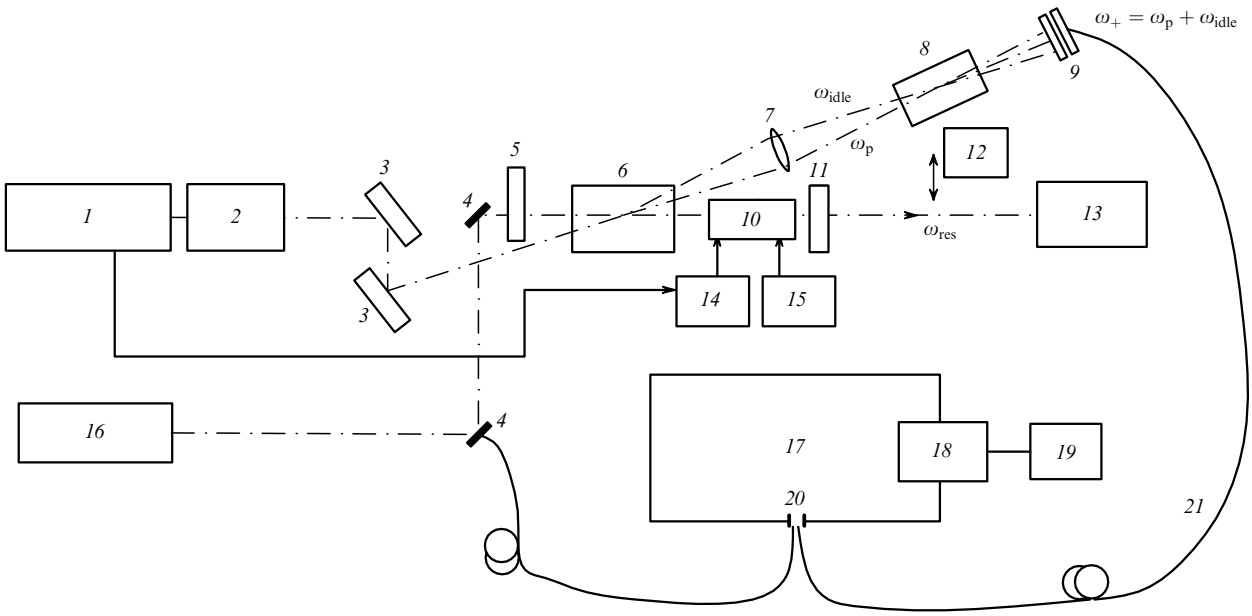

Figure 1. Schematic of the experimental facility for the investigation of an OPO with an AOD and an AOF: (*1*) pump laser; (*2*) AOD; (*3, 4, 5, 11*) mirrors; (*6*) nonlinear $LiNbO_3$ crystal; (*7*) lens; (*8*) nonlinear KTA crystal; (*9*) filters; (*10*) AOF unit; (*12*) energy meter; (*13*) Digikrom CM 112 spectrometer; (*14*) G5-54 oscillator; (*15*) driver; (*16*) alignment laser; (*17*) spectrum analyser; (*18*) video camera; (*19*) picture monitor; (*20*) vertical slit; (*21*) optical fibre bundle.

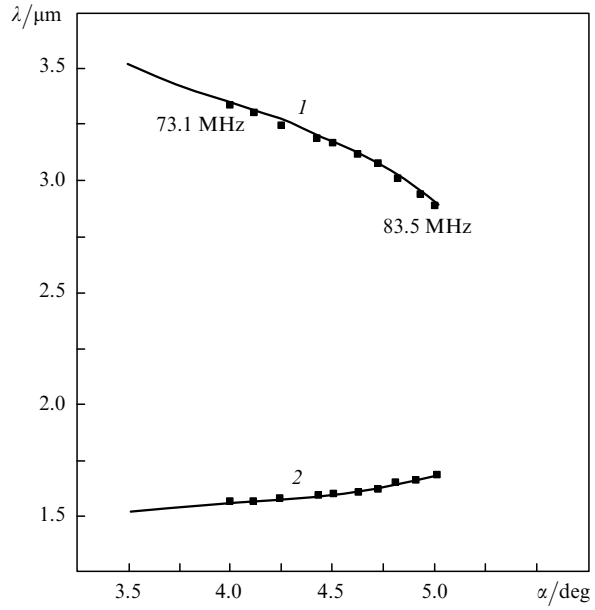

Figure 2. OPO tuning curves for the cavity (*1*) and idle (*2*) waves and experimental points.

Expanding the angular spectral tuning range to 2° requires making special-purpose optics in order to transfer the pump-beam rotation axis from the AOD centre to the centre of the OPO crystal.

Investigation of the spectral radiation characteristics of the OPO with the AOF. Based on the scheme of quasicollinear acoustooptical interaction in a TeO_2 crystal, we designed a filter with the narrowest possible instrumental function, which was limited only by the dimensions and uniformity of the crystal [10].

The main technical characteristics of the AOF were as follows: a 2–4 μm optical tuning range, a transmission coefficient of no less than 90 % in the tuning range, a tuning step of 0.5 cm^{-1}, the time of setting the desired wavelength was within 100 μs throughout the tuning range, the precision of setting the desired wavelength of 0.1 cm^{-1}, the spectral drift of the beam axis was within the diffraction angle and the depolarisation within 1 %, and the acousto-optical interaction length was 45 mm. Control was exerted by a driver from an IBM PC via a parallel port.

To calibrate the work AOF specimen, we measured the acoustic wave frequency corresponding to the filtration of 3.39-μm radiation. The 3.39-μm radiation was provided by an LGN 118-3V He–Ne laser. The acoustic frequency was determined whereby there occurred filtration at the 3.39 μm wavelength; it was equal to 22780 kHz. It is pertinent to note that the acoustic frequency corresponding to a fixed wavelength depends on the AOF design version; for the previous AOF specimen, for instance, it was equal to 22641 kHz. Proceeding from the measurements of the filtration wavelength λ as a function of acoustic frequency f_s, we plotted the calibration curve of the work AOF specimen (Fig. 3).

At the 3.39-μm wavelength we also measured the diffraction efficiency T and the one-pass instrumental width $\Delta\lambda_{0.5}$, which were equal to 95 % and 1.7 cm^{-1}, respectively. In the conditions of OPO lasing, the AOF instrumental width should become $P^{1/2}$ times narrower, where P is the number of radiation passes in the cavity.

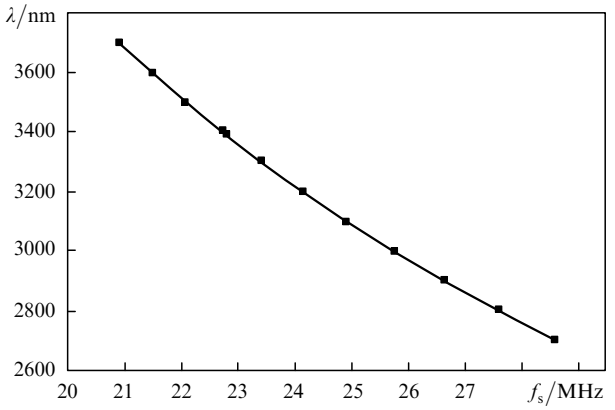

Figure 3. Calibration curve of the work AOF specimen.

With the use of the infrared AOF developed, we recorded the natural (unnarrowed) line shapes of OPO lasing, i.e. the AOF served as a spectrum analyser. Figure 4 shows OPO output lines normalised to the maximum intensity I, which were recorded for different optical axis orientations of the $LiNbO_3$ crystal in the collinear (2402, 2470, and 2502 nm) and noncollinear (3320 nm) setups. Figure 5 shows the shape of the OPO output 3320-nm line, normalised to the intensity I, expressed in terms of the acoustic frequency with the help of the AOF.

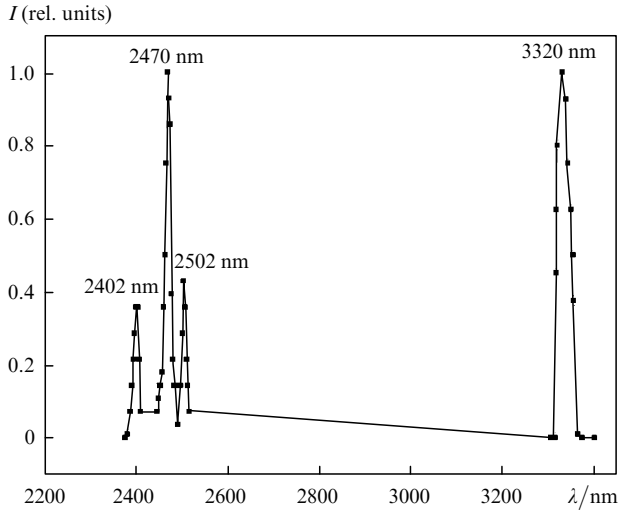

Figure 4. OPO output line shapes recorded with the help of the AOF.

The effect of narrowing of the lasing line of a collinear OPO with the help of an intracavity AOF was first reported in our work [6]. Measurements were made of the width of the lasing band at a wavelength of 2500 nm. The output radiation was recorded with the help of a system based on a modernised MDR-23 monochromator. The modernisation involved extending the operating range of the monochromator to the IR range and automating its tuning (by a motor with a reduction unit) with the simultaneous recording of the output energy by a PbS photodiode and computer information storage. We recorded the narrowing of the output lasing line from 20 cm^{-1} to 5 cm^{-1} – the value limited by the resolution of the spectral instrument involved.

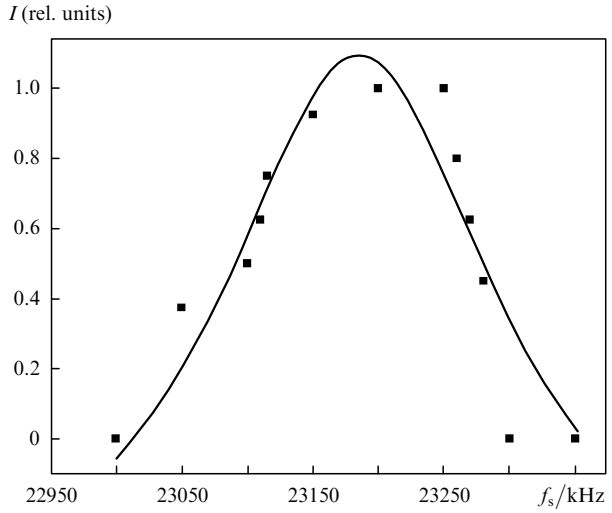

Figure 5. Shape of the OPO 3320-nm lasing line plotted in terms of acoustic frequencies using the AOF (points); the solid curve is a Lorentzian approximation function.

In the experiment conducted in the present work, for the noncollinear OPO operating at a wavelength of 3340 nm (3010 cm^{-1}) we observed on the screen of the picture monitor (*19*) (see Fig. 1) a more than a 10-fold narrowing of the lasing line on placing the AOF into the OPO cavity and estimated its width. The natural width of the lasing line of visualised 633-nm radiation was measured at ~ 40 cm^{-1}, while the width of the line narrowed with the help of the intracavity AOF was measured at about 3 cm^{-1}. In this case, account should be taken of the fact that visualised in this experiment was the shorter-wavelength 1561-nm output radiation, whose spectral width, unlike the 3340-nm radiation, was increased due to the divergence of the pumping radiation (by approximately 1.5 cm^{-1}, according to our estimates). Furthermore, the line width of the pump radiation (1 cm^{-1}) makes its own contribution to the line width of the sum frequency (of the visible range). Proceeding from our experimental data we estimate the line width of the cavity 3340-nm wave at 0.5–0.8 cm^{-1}, which is in good agreement with the AOF instrumental width calculated for our scheme (0.6 cm^{-1}). We plan to perform experiments to directly measure the cavity line width of the OPO with an intracavity AOF at some future date.

2.2 OPO with a BBO single crystal and an electrodynamic output frequency tuning

The rate of OPO wavelength tuning by way of rotation of the nonlinear crystal in the cavity is determined primarily by the rate of angular crystal rotation and the steepness of its tuning characteristic. In the known schemes of commercially available BBO-based lasers, the frequency tuning is effected sequentially, using a micrometer feed and a mechanical unit, or, to raise the rate, by rotating a micrometer screw with the help of a computer-controlled step motor.

In our work the further improvement of the tuning rate was achieved by employing fast-acting electrodynamic drives (EDDs). In this case, the nonlinear crystals in their mounts were accommodated directly on the axes of the EDD executive devices. This provided the high angular rate of crystal position variation and, as a consequence, the high rate of output wavelength tuning.

We developed and investigated a fast-tunable OPO of the visible and near-IR ranges (0.47–1.5 μm). Use was made of a well-known collinear OPO scheme with two identical (cut out of a common boule) nonlinear BBO crystals. The crystals were oriented in such a way as to cancel out the 'drift' of the pumping energy and thereby substantially lengthen the interaction path and hence improve the OPO efficiency. 'Fast' wavelength tuning in the 0.47–1.5-μm range was effected for each of the BBO crystals by means of two identical single-coordinate EDDs.

Technical characteristics of the EDDs developed: load dimensions (BBO crystal) were $12 \times 12 \times 14$ mm, the load mass was 50 g, and the angular range of crystal rotation was $\pm 2.5^\circ$; on application of a control signal in the form of a rectangular pulse (in the independent mode), the process rise time was equal to 2 ms and the settling time (corresponding to the wavelength tuning time) was 5 ms. The angular mismatch of the positions of the two EDDs in the tuning throughout the spectral range did not exceed the value corresponding to the output radiation bandwidth. Furthermore, the code developed for controlling the EDDs permitted specifying an arbitrary sequence of the wavelengths to be generated, which is of significance when employing an OPO in DA lidars.

3. Chalcogenide-crystal OPO and new type of solid-solution OPO tuning

OPO based on an $AgGaS_2$ single crystal. The OPO intended for the middle-IR range was developed for solving the task of detection of methane and other light hydrocarbons by the DA technique [5]. A common feature of these substances is the presence of molecular C–H groups in their chemical structure and characteristic absorption lines (3–5 μm) in the middle-IR range.

In the present work we investigated the frequency tuning of a nanosecond OPO based on a silver thiogallate ($AgGaS_2$) crystal, which exhibits strong nonlinearity ($d_{36} = 22$ pm V^{-1}), low absorption ($\alpha \leqslant 0.07$ cm^{-1}) in the 3.0–5.0-μm range, nonhygroscopicity, and temperature stability. In our experiments the angle of pump radiation incidence on the input cavity mirror was varied by rotating the OPO cavity as a whole (in the future we plan to make use of a high-speed AOD for changing the angle of pump incidence for an immobile cavity, which was realised in the $LiNbO_3$-based OPO described above).

The OPO was made according to a one-cavity scheme with an 18-mm-long $AgGaS_2$ crystal with an aperture of 10×10 mm and was pumped by the radiation of an Nd : YAG laser with a wavelength of 1.064 μm and a pulse repetition rate of 12.5 Hz. A set of aperture stops enabled extracting one transverse mode from the pump radiation. The cavity was realised for the 'short' wavelength of the parametric pair and comprised two plane mirrors with $R = 91\,\%$ in the 1.5–1.8-μm range. In the experiment, when the angle between the pump radiation direction and the cavity axis was varied within 3.5° in the air, the output wavelength varied from 3.0 to 3.6 μm. In this case, the angle of inclination of the optical crystal axis relative to the cavity axis was equal to 51°.

OPO based on an $HgGa_2S_2$ single crystal. The main results of a series of experimental investigations of an OPO with a mercury thiogallate crystal pumped by a pulse-periodic Nd : YAG laser were published in Refs [8, 9].

Bodice et al. [9] made use of an $HgGa_2S_4$ crystal grown by a Bridgman–Stockbarger technique in High Technologies Laboratory of Kuban State University. The specimen measured 10.1 mm in length, 13.8 mm in height, and 13.3 mm in width; it was cut at an angle $\theta = 52.7^\circ$ with respect to the crystal axis, which was oriented for the type-I phase matching. Deposited on the working faces of the crystal was a dielectric coating with a reflectivity below 2 % for the pump radiation with a wavelength $\lambda = 1.064$ μm and below 0.5 % for the 1.2-1.4-μm radiation (the signal wave).

For a pump source we used an off-the-shelf Nd : YAG laser with a Gaussian profile of cavity mirror reflectivity (Quintal, Brio model). The laser operated at a wavelength of 1.064 μm in the pulse-periodic mode with a pulse repetition rate of up to 20 Hz; the pulse energy was equal to 100 mJ for a stability of ±2 %. The half-amplitude pulse duration (FWHM) was equal to 4.5 ns, the radiation divergence did not exceed 0.3 mrad. To ensure against optical crystal damage, a two-power telescope was introduced into the setup to increase the pump beam diameter to 6 mm (at a $1/e^2$ level).

The wavelength tuning range achieved experimentally for the idle radiation was 3.69–5.69 μm. In this case, the exterior angle of crystal rotation was equal to 20°. The spectral width of the tuning range was determined by mirror reflectivities and crystal dimensions.

Badikov et al. [9] presented the wavelength dependence of the average OPO output (the highest value was obtained for $\lambda = 4.03$ μm when the pump radiation was normally incident on the crystal) and the dependence of series-averaged OPO pulse energy on the average energy of the pump pulses (the highest series-averaged output OPO pulse energy was equal to 3.3 mJ). In this case, the energy conversion efficiency was 4.7 % and the differential conversion efficiency was 4.9 %.

The duration of OPO output pulses at a wavelength of 4.03 μm turned out to be virtually equal to the duration of the pump pulses and was equal to ~ 3 ns (FWHM). The delay of OPO lasing relative to the pump radiation was equal to 1 ns.

The intensity OPO 4.03-μm radiation distribution over the beam section was measured by a Pyrocam III camera. The radiation divergence was estimated at ~ 10 mrad.

OPO based on the solid solutions of composition $Hg_{1-x}Cd_xGa_2S_4$. Addition of cadmium to $HgGa_2S_4$ crystals permits producing cadmium–mercury thiogallate solid solutions of composition $Hg_{1-x}Cd_xGa_2S_4$, which offer a number of advantages.

First, the introduction of cadmium at different densities results in changes of the birefringence and the principal values of the refractive index in crystals. As a result, by varying the magnitude of x it is possible to control the phase matching conditions. In particular, for certain cadmium densities in the crystal it is possible to realise the conditions for an uncritical phase matching.

Second, in the course of crystal growth there emerges a natural cadmium density gradient along the boule length. This circumstance permits making the elements for nonlinear-optical converters with a smooth x variation in the phase matching plane. With the use of these elements it is possible to tune the OPO wavelength by way of linear crystal translation relative to the pump beam (or pump beam translation relative to the crystal). In doing this, the uncritical phase matching conditions are not violated.

Due to the development of the technology of single crystal growing by Bridgeman–Stockbarger technique in the High Technologies Laboratory of Kuban State University, it has been possible to grow a high-quality $Hg_{1-x}Cd_xGa_2S_4$ crystal with a smoothly varying cadmium density in the phase matching plane [7]. An 11-mm-long element with a transverse section of 30.6×8 mm was cut from this crystal; the element was oriented for the realisation of type-I uncritical phase matching (e–oo) ($\theta = 90^\circ$, $\varphi = 45^\circ$). An insignificant colour variation from one face to the other was observed along the optical axis of the crystal. Antireflection coatings were deposited on the optical surfaces of the element. The reflectivities of each surface were 0.2 % – 0.8 % in the 1–2-μm spectral range.

For an OPO pump source, use was made of an Nd : YAG laser with a ring semiconfocal cavity, which provided lasing in a travelling wave mode. The lasing was effected under Q-switching. An aperture stop 1.7 mm in diameter located inside the ring cavity ensured lasing by the fundamental TEM_{00} mode. The half-amplitude duration of output pulses was 22 ns, the peak energy of a single pulse amounted to 12 mJ. The laser operated in a pulse-periodic mode with a frequency of up to 10 Hz.

The OPO cavity was formed by two plane mirrors with dielectric coatings. The input OPO mirror with an antireflection coating for the pump radiation on the front surface was made of KV quartz glass and the output one of calcium fluoride. The reflectivities of the input and output mirrors were 95 %–99 % in the 1.4–1.9 μm range. Therefore, the cavity Q-factor was highest for the signal wave, and the idle wave was extracted from the cavity with a minimum loss (the output mirror transmittance was 80 %–90 %). For the pump radiation, the reflectivity of the input mirror was 10 % and the reflectivity of the output mirror was 30 %. The OPO cavity mirrors were spaced at 3 cm. The OPO was located in the pump beam waist formed by a focusing mirror ($F = 2$ cm). The beam waist diameter at a $1/e^2$ level was equal to 2 mm in the region of interaction with the crystal. The output wavelength was tuned by way of linear translation of the crystal relative to the pump beam in the direction of its axis.

To measure the pump pulse energy and the distribution of intensity over the beam section, a part of the radiation was diverted using an optical wedge and measured with a PE-10-BB energy meter (Ophir) and a C4915 camera (Cohu). The OPO output energy was measured with the PE-10-BB energy meter, the idle wave was extracted using a set of calcium fluoride filters with a dielectric coating (with transmittance below 1 % for the pump radiation) and a germanium plate. A Digikrom CM112 monochromator was employed for wavelength measurements. The signal transmitted through the monochromator was recorded with an MG-30 pyroelectric device and a TDS-1012 oscilloscope. The OPO radiation was focused by a barium fluoride lens with a focal length of 60 mm. Wavelengths were measured accurate to 0.01 μm. A Pyrocam-III camera (Spiricon) was employed to monitor the spatial distribution of radiation intensity over the beam section both for the idle and signal waves.

The following parameters were measured in our work: the OPO output energy E_{idle} at the frequency of the idle wave, the pump radiation energy E_p and the idle radiation wavelength λ_{idle}. The energy conversion efficiency $\eta = E_{idle}/E_p$ was determined from the measurements of E_p

and E_{idle} The differential conversion efficiency η_{slope} was determined from the slope of approximation dependence $E_{idle}(E_p)$.

We obtained parametric lasing from a cadmium–mercury thiogallate crystal for the first time. The range of continuous wavelength tuning was 2.85–3.27 μm. The threshold pumping energy for different crystal positions was 2.5–4 mJ. Figure 6 shows the output OPO energy at the frequency of the idle wave as a function of pumping energy. The highest energy conversion efficiency for the idle wave ($\lambda_i = 3.03$ μm) was 4.5 %, the differential conversion efficiency amounted to 6.6 %.

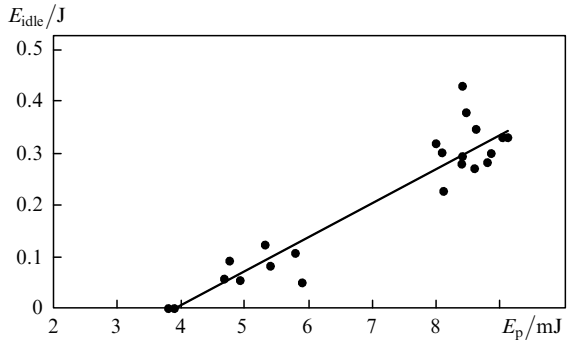

Figure 6. Output OPO energy at the frequency of the idle wave versus pumping radiation energy ($z = 11$ mm).

Figure 7 depicts the measured energy conversion efficiency and the differential conversion efficiency as functions of the pumping beam position. For $z = 0 - 25$ mm they vary over relatively narrow limits, which is testimony to the uniformity of cadmium distribution along the crystal axis. One can see that the conversion efficiency lowers substantially in the edge crystal region (~ 3 mm). This is supposedly due to significant distortions of the phase composition in this region.

Measurements were made of the near- and far-field spatial radiation intensity distributions over the section of the idle wave beam (Fig. 8). From the analysis of these distributions it is possible to judge the optical quality of the crystal. By and large the resultant OPO intensity distributions suggest that the uniformities of refractive index distribution in the crystal are insignificant, at least in the

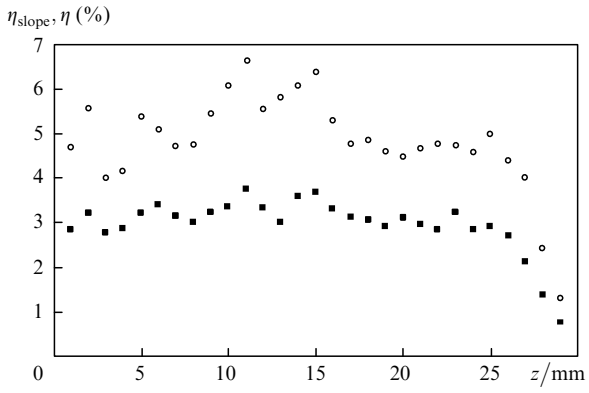

Figure 7. Dependence of the maximum (■) and differential (○) energy conversion efficiencies on the pump beam displacement relative to the lateral surface of the crystal (in the phase matching plane).

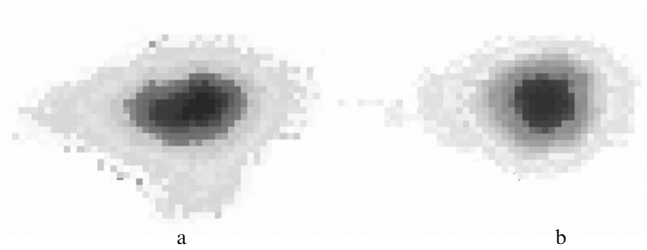

Figure 8. Near-field (the distance from the output OPO mirror is 160 mm) (a) and far-field (at the focus of a lens with a focal length of 100 mm) intensity distributions over the beam section at the OPO output at the idle wave frequency ($\lambda_{idle} = 3.03$ μm) for $z = 11$ mm.

volume of wave interaction. The elongated shape is supposedly due to the spreading of radiation in the phase matching plane. The divergence of the idle OPO radiation wave was $\sim 2 \times 10^{-2}$ rad at a $1/e^2$ level.

Figure 9 shows the experimentally determined dependence of the idle radiation wavelength on the position of the pumping beam in the crystal. Shifting the beam in the phase matching plane by 28 mm changed the wavelength by 0.42 μm.

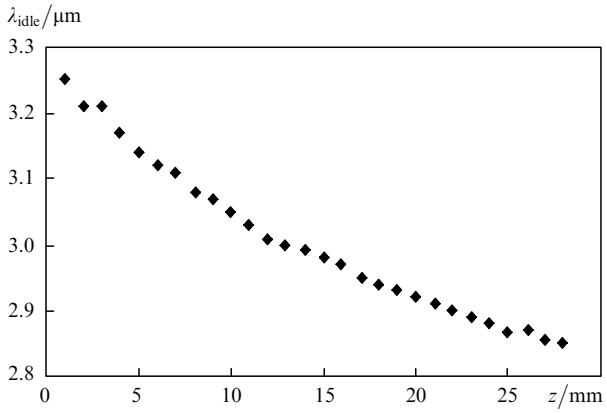

Figure 9. Idle radiation wavelength at the OPO output as a function of pump beam displacement relative to the side surface of the crystal.

To determine the relation between the chemical composition of the $Hg_{1-x}Cd_xGa_2S_4$ crystal and its optical properties we performed measurements of the dispersion of refractive indices. To this end, prisms with $x = 0.27$ and 0.23, a prism angle of $\sim 20^\circ$, and prism faces measuring 10×10 mm were prepared. The refractive indices were measured in the 0.55–10-μm range by an autocollimation technique using a facility described in Ref. [11]. To approximate the resultant values of refractive index, advantage was taken of Sellmeier equation [12, 13]

$$n^2 = A_1 + \frac{A_3}{A_2 - \lambda^2} + \frac{A_5}{A_4 - \lambda^2}, \qquad (1)$$

where λ is the radiation wavelength in micrometers. To determine Sellmeier coefficients A_{1-5} for other cadmium densities, use was made of refractive indices found by interpolating in x the dependences $n_o(\lambda)$ and $n_e(\lambda)$ for $x = 0.27$ and 0.33 as well as similar dependences measured in Refs [13, 14]. The Sellmeier coefficients determined in this way for crystals with different cadmium densities are collected in Table 1.

Table 1. Sellmeier coefficients for $Hg_{1-x}Cd_xGa_2S_4$ solid solutions.

x	n	A_1	A_2	A_3	A_4	A_5
0.20	n_o	7.17117	639.04	−914.648	0.0979835	−0.220006
	n_e	7.03365	653.431	−943.36	0.0770492	−0.210144
0.25	n_o	7.42819	749.29	−1295.98	0.0880175	−0.219608
	n_e	7.3628	783.563	−1411.87	0.0801083	−0.207095
0.30	n_o	7.62356	836.474	−1642.64	0.0717384	−0.220695
	n_e	7.41107	805.268	−1512.04	0.0714881	−0.207339
0.35	n_o	8.47402	1167.86	−3327.19	0.0635593	−0.2180798
	n_e	8.40374	1171.46	−3389.17	0.0807452	−0.2007114
0.40	n_o	8.47346	1184.47	−3414.44	0.0406186	−0.220462
	n_e	8.33498	1143.19	−3255.20	0.0705351	−0.20029
0.45	n_o	8.50139	1213.14	−3569.69	0.0180232	−0.221991
	n_e	8.45613	1182.89	−3536.20	0.0653473	−0.197853
0.50	n_o	8.47455	1222.13	−3599.99	−0.00379508	−0.222829
	n_e	8.42368	1168.94	−3479.53	0.0602277	−0.19524

The maximum departure of the values of refractive index obtained through approximation from experimental data is equal to 3×10^{-3}.

The cadmium densities in the crystal were determined employing the resultant Sellmeier equations and the wavelengths calculated on their basis for the 90° phase matching conditions. For points $z = 0$ and 28 mm, the cadmium density x was equal to 0.25 and 0.21, respectively. Figure 10 shows the dependence of the cadmium density on the displacement of the pumping beam in the phase matching plane, which was determined from the experimental data for the idle wavelength. An analysis of the dependence plotted in Fig. 10 suggests that the cadmium density varies smoothly over the length of the element, this dependence being close to a linear one. This is additional indication that the optical quality of the crystal is high.

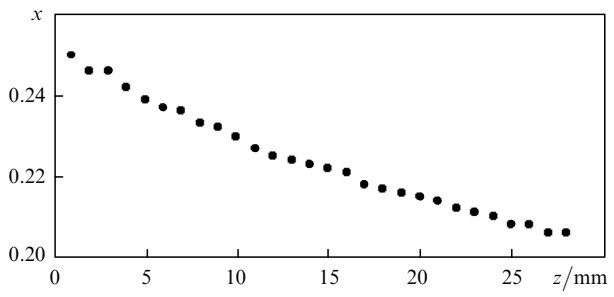

Figure 10. Calculated cadmium density in the crystal as a function distance to the side crystal surface.

4. Conclusions

The following results were obtained in the investigation of the ways of tuning OPOs of the visible and near-IR ranges.

In the experiment involving a paratellurite-based acoustooptical deflector, the range of acoustic AOD frequency variation was 73.1 – 83.5 MHz; in this case, the wavelengths of OPO output were tuned in the 1.56 – 1.69-μm and 3.36 – 2.88-μm ranges. The time required for setting a desired wavelength was equal to ~ 0.1 ms. Scanning was performed over a range of 1°; extending the angular spectral tuning range to 2° calls for the making of special optics to transfer pump-beam rotation axis from the AOD centre to the centre of the OPO crystal.

An investigation was made of schemes with an acousto-optical filter on the basis of paratellurite. On placing the AOF inside the OPO cavity we observed a narrowing of the spectral width of the OPO output line by more than a factor of 10. The experiments conducted in our work have demonstrated the feasibility of employing an acoustooptical filter in a middle-IR OPO both for narrowing its lasing band (for an intracavity location of the AOF) and for analysing the output OPO spectrum (for an extracavity location of the AOF). The AOD and the AOF intended for the 2 – 4-μm range, which were employed in our experiments, were made at the VNIIFTRI.

We have developed and investigated a BBO-crystal based OPO for the visible range; its wavelength tuning is effected by two automatic drives involving electrodynamic actuators. The time required for radiation wavelength tuning in the 0.47 – 1.5-μm range was measured at 5 ms. The sequence of the output wavelengths to be generated may be arbitrary.

We have made OPOs based on chalcogenide crystals (silver and mercury thiogallates), which are pumped by Nd : YAG laser radiation and are continuously tunable in the 3.0 – 5.7-μm wavelength range.

A technology was developed and a new nonlinear crystal, cadmium – mercury thiogallate ($Hg_{1-x}Cd_xGa_2S_4$), was grown; the crystal possesses a high optical quality and a uniform Cd impurity distribution along its optical axis. As a result, on the basis of this crystal it has been possible to make an OPO pumped by Nd : YAG laser radiation, which operates in the regime of uncritical phase matching and relies on a radically new technique of continuous wavelength tuning in the middle-IR range – by way of varying the density parameter x. The tuning range was 2.85 – 3.27 μm and the highest differential conversion efficiency was 6.6 %. The range of continuous OPO wavelength tuning was limited only by the density of Cd. By varying parameter x from 0.14 to 0.56 it is possible to obtain tuneable OPO lasing in the conditions of uncritical phase matching in the 2.7 – 9-μm range.

References

1. Babin A.A., Karov A.V., et al. *Prib. Tekh. Eksp.*, **3**, 160 (1989).
2. Ewbank M.D., Rosker M.J., Bennett G.L. *J. Opt. Soc. Am. B*, **14**, 666 (1997).
3. Egret G., Fix A., Weiss V., Poberaj G., Baumert T. *Appl. Phys. B*, **67**, 427 (1998).
4. Sjöholm M., Weibring P., Edner H., Svanberg S. *Opt. Express*, **12** (4), 554 (2004).
5. Andreeva N.P., Barashkov M.S., Demkin V.K., Pshenichnikov S.M., in *Oboronnyi kompleks–naucho-tekhnicheskomu progressu Rossii* (Defence Industry's Contribution to Russia's Scientific and Technological Advance) (Moscow: Izd. VIMI, 1996) No. 3, p. 87.
6. Andreev S.A., Andreeva N.P., Barashkov M.S., Demkin V.K., et al., in *Akustoopticheskie, akusticheskie i rentgeno-spektral'nye metody i sredstva izmerenii v nauke i tekhnike* (Acoustooptical, Acoustic, and X-Ray Spectral Methods and Measurement Instrumentation in Science and Technology (Moscow: Izd. VNIIFTRI, 2005) Issue No. 48 (140), p. 35.
7. Badikov V.V., Don A.K., Mitin K.V., Seregin A.M., Sinaiskii V.V., Shchebetova N.I. *Kvantovaya Elektronika*, **35**, 853 (2005) [*Quantum Electron.*, **35**, 853 (2005)].
8. Badikov V.V., Don A.K., Mitin K.V., Seregin A.M., Sinaiskii V.V., Shchebetova N.I. *Kvantovaya Elektronika*, **33**, 831 (2003) [*Quantum Electron.*, **33**, 831 (2003)].
9. Badikov V.V., Don A.K., Mitin K.V., Seregin A.M., Sinaiskii V.V., Shchebetova N.I., Shchetinkina T.A. *Kvantovaya Elektronika*, **37**, 363 (2007) [*Quantum Electron.*, **37**, 363 (2007)].
10. Chang I.C. *Electron. Lett.*, **28**, 1255 (1992).
11. Badikov V.V. et al. *Opt. Mater.*, **23**, 575 (2003).
12. Badikov V.V., Kuz'min N.V., Laptev V.B., et al. *Kvantovaya Elektronika*, **34**, 451 (2004) [*Quantum Electron.*, **34**, 451 (2004)].
13. Badikov V.V., Matveev I.N., Panyutin V.L., et al. *Kvantovaya Elektronika*, **6**, 1807 (1979) [*Sov. J. Quantum Electron.*, **9**, 1068 (1979)].
14. Badikov V.V., Matveev I.N., Pshenichnikov S.M., Rychik O.V., Trotsenko N.K., Ustinov N.D. Inventor's Certificate No. 974810. Invention Application No. 3214481. Priority date 4.12.1980.